Bifurcation instability and chute cutoff development in meandering gravel-bed rivers

W.M. van Dijk, F. Schuurman, W.I. van de Lageweg, and M.G. Kleinhans

Faculty of Geosciences, Department of Physical Geography, Utrecht University, Utrecht, The Netherlands.
woutvandijk@gmail.com

Abstract

Chute cutoffs reduce sinuosity of meandering rivers and potentially cause a transition from a single to a multiple channel river. The channel bifurcation of the main channel and the mouth of the incipient chute channel controls sediment and flow partitioning and development of the chute. Recent channel bifurcation models suggest that upstream bend radius, gradient advantage, inlet step, and upstream sediment supply at the bifurcation are important factors in the evolution of bifurcations. Our objective is to unravel the relative importance of these factors for chute cutoff success and development. We compare results from a morphodynamic three-dimensional (3D) model and a one-dimensional (1D) model with nodal-point relation with field observations of chute cutoffs in a meandering gravel-bed river. The balance between increased gradient advantage and flow curvature upstream of the chute channel bifurcation was systematically investigated with the 1D model. The 3D model runs and the field observations show the development of two types of chute cutoffs: a scroll-slough cutoff and a bend cutoff. The morphodynamic 3D model demonstrates that chutes are initiated when flow depth exceeds the floodplain elevation. Overbank flow and a significant gradient advantage result in a bend cutoff. The outcome of the 1D model shows that channel curvature at the bifurcation determines the success or failure of the chute cutoff when the chute channel is located at the inner bend, as in the case of scroll-slough cutoffs. We conclude that chute initiation depends on floodplain characteristics, i.e., floodplain elevation, sediment composition, and the presence of vegetation. Chute cutoff *success* or *failure* is determined by the dynamics just upstream of the channel bifurcation and location of the chute channel in the bend, which determines channel curvature and gradient advantage. These findings have ramifications for the prediction of chute cutoff in a wide range of rivers under natural and managed conditions and for the understanding of stratigraphy and architecture of deposits.

1. Introduction

River bifurcations are found in rivers across a large range of scales, from flow around a bar to a splitting river at the delta apex. River bifurcations are crucial elements in many rivers (Kleinhans et al., 2013): multithread anastomosing rivers (Kleinhans et al., 2012), chute cutoffs in meandering rivers (Grenfell et al., 2012), and braid bars in braided rivers (Ashmore, 1991; Federici and Paola, 2003; Zolezzi et al., 2009). Empirical classifications of channel patterns (Kleinhans and van den Berg, 2011) suggest a close association of chute cutoffs with meandering river styles at the transition to braiding. A *chute cutoff* develops by a shortcut over a point bar and is presently more difficult to predict than a *neck cutoff*, which occurs when two migrating bends intersect (Howard, 1996). Understanding the controls on chute cutoffs and the stability of the bifurcate meander bends may yield insight into the transition between braided and meandering rivers (e.g., Marston et al., 1995; Grenfell et al., 2012). Furthermore, the understanding of chute cutoffs is essential for understanding stratigraphy (McGowen and Garner, 1970). The process of chute cutoffs reduces the discharge through the main channel and as result decreases outer bank erosion (Hooke, 2003; Kleinhans et al., 2011; Grenfell et al., In press). Furthermore, chute cutoffs locally increase the sediment load causing deposition elsewhere, which affects navigation through the river (Zinger et al., 2011). Recently, significant progress was made in understanding the dynamics of chute cutoffs in field studies (Constantine et al., 2010b; Micheli and Larsen, 2011; Grenfell et al., 2012), while morphodynamic models have remained underemployed for this purpose (Howard, 1996; Zolezzi et al., 2012). Here we study the controlling factors for initiation and development of chute cutoffs based on field observations, a morphodynamic three-dimensional (3D) model, and a one-dimensional (1D) model with a nodal-point relation for the partitioning of flow and sediment.

Field studies described the initiation of chute cutoffs either by headward incision of a channel that captures an increasing volume of the overbank flow (Gay et al., 1998; Zinger et al., 2011), extend downstream from an erosional embayment (Constantine et al., 2010b), or a combination of both processes (Kleinhans and van den Berg, 2011). Conceptually, distinguishing two types of chute cutoffs is useful: (i) scroll-slough cutoffs through sloughs on point bars (Fisk, 1947; Grenfell et al., 2012), or (ii) a bend cutoff across the point bar by incision. Sloughs form where inner-bank attachment of scroll bars is inter-

rupted. Floods usually trigger chute cutoff, which requires high water levels and high rates of bed load transport unlike neck cutoff (Lewis and Lewin, 1983; Howard, 1996; Ghinassi, 2011; Zinger et al., 2011). Following a successful chute cutoff, the reduced sediment transport capacity in the abandoned branch is smaller than the supply that leads to closure by a sandy plug bar (Constantine et al., 2010a; van Dijk et al., 2012). Later, the residual channel is slowly filled by overbank flow and deposition of fine material (Toonen et al., 2012; Dieras et al., 2013).

Bifurcation development is determined by the division of water and sediment to the downstream branches in relation to their conveyance and transport capacity (Wang et al., 1995; Bolla Pittaluga et al., 2003; Hardy et al., 2011). The division of water and sediment between both branches can change over time as a result of change of the downstream branches, for example channel widening (Miori et al., 2006) or lengthening. Also, conditions in the upstream channel affect the partitioning: particularly helical flow because of curvature, presence of bars (Kleinhans et al., 2011), and inlet steps (Bertoldi et al., 2009) that cause gravity-driven sediment deflection on the transversely sloping bed (Bolla Pittaluga et al., 2003; Kleinhans et al., 2008). When sediment input into the downstream branches, determined by the partitioning at the bifurcation, differs from sediment transport capacity in the downstream branches, determined by the downstream conditions, then one of the branches will close (Constantine et al., 2010a; Kleinhans et al., 2011). The division of discharge and sediment at the bifurcation is described in several nodal point relations (e.g., Wang et al., 1995; Bolla Pittaluga et al., 2003; Kleinhans et al., 2008). Bifurcation asymmetry is determined by the inlet steps, i.e., bed level difference between both branches at the upstream branch (Bertoldi et al., 2009) and gradient advantage of one downstream branch. The transverse bed slope and curvature-driven helical flow — related to bend radius — have a significant effect on the division of bedload sediment between both branches in meandering rivers (Kleinhans et al., 2008). This suggests that chute cutoff processes may also be affected by upstream channel curvature.

The rate of channel closure depends on the bifurcation angle between the chute and main branch (Constantine et al., 2010a). A large bifurcation angle leads to rapid decrease of the channel width of the former main branch. However, van der Mark and Mosselman (2013) showed that the bifurcation angle seems not to affect the sediment division significantly. The problem is that a bifurcation angle may appear as sharp at the scale of maps or aerial photography. Indeed for very sharp corners a bifurcation angle may be indicative of highly 3D situations with flow separation (Constantine et al., 2010a; Blanckaert, 2011), but when flow is more gently curved the bifurcation is more appropriately described by curvature as a proxy for helical flow structure and its effects on sediment transport (van der Mark and Mosselman, 2013; Kleinhans et al., 2013). Here we show that the closure rate is predictable from relative bend radius and the normalized chute channel length.

The objective of this paper is to assess the effects of upstream channel curvature, gradient advantage, inlet steps, and sediment load division on bifurcation initiation and development of chute cutoffs. Here we used morphodynamic modelling (Delft3D) of a dynamic meandering gravel-bed river that exhibits chute cutoffs to quantify the necessary conditions for chute cutoffs. We also use the 1D model of Kleinhans et al. (2011) to systematically explore in a large number of runs the combined effects of upstream channel curvature and gradient advantage across the potential cutoff channel. We compare the 3D model results with field observations, experiments, and the 1D-nodal-point model (described in Kleinhans et al., 2011). The idealized model setup was inspired by the River Allier, which is a meandering gravel-bed river dominated by chute cutoffs, and by our scale experiments (van Dijk et al., 2012).

2. Recent history of channel planform dynamics

The River Allier upstream of the city of Moulins (France) is a dynamic meandering gravel-bed river with chute cutoffs on the transition from scroll bar and neck cutoff-dominated meandering rivers to weakly braided rivers (river nr. 112 in the data set in Kleinhans and van den Berg (2011), see their Fig. 13). Here the maximum reach-averaged sinuosity is 1.5 with bend migration rates up to 60 m/y. The River Allier flows in a valley with a gradient of 3.3 m/km and is a tributary of the River Loire in central France (46°29′53″N., 3°19′38″E.). It is a rain-fed river with a flashy hydrograph and a mean annual discharge of 140 m^3/s and mean annual flood discharge of 500 m^3/s. Table 1 indicates the flood frequency that is based on data collected between 1986 and 2012.

Table 1: *Flood occurrence Allier at Chatel-de-Neuvre for 1986–2012*

Recurrence interval (y)	Discharge (m^3/s)
2	620
5	880
10	1100
20	1200

Bend migration and chute cutoffs perpetually changed the meander planform. The River Allier became temporarily weakly braided after a bridge was built and a high flood peak led to cutoffs of several channel bends in 1980 (Fig. 13 in Kleinhans and

van den Berg, 2011). The event with multiple simultaneous chute cutoffs occurred once, whereas single-bend cutoffs occurred frequently. Gradient advantage for these cutoffs varied (Table 2, 1–4). For example, the current channel and remnants of former channels shown in Fig. 1 at Tilly were formed because of several flood events in 1994, 2003, and 2008, which all led to single-bend cutoffs. Here, the chute channel was more than twice as short as the main meander channel (Table 2, 5–7). After cutoffs, new meander bends developed and increased the sinuosity of the river.

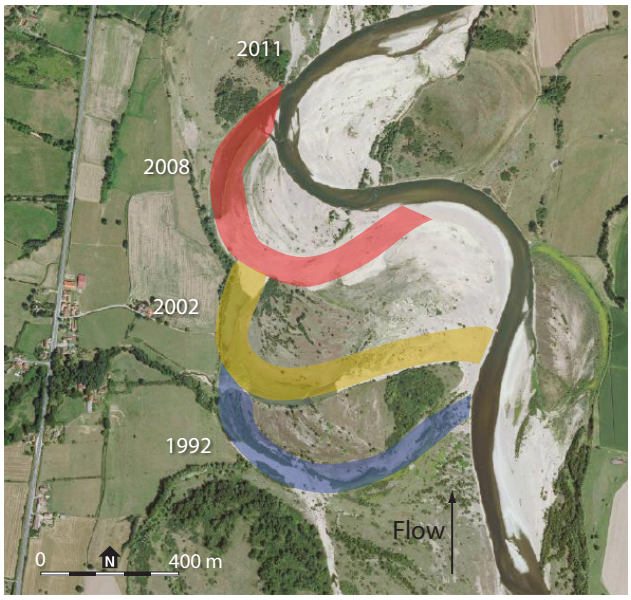

Figure 1: *Aerial image of the River Allier shows several former channels that were abandoned by chute cutoffs that could be related to flood events. Flood peaks on 8 November 1994 (1020 m^3/s), 6 December 2003 (1370 m^3/s), and 5 November 2008 (850 m^3/s) all led to major cutoffs (source: IGN-France and Ministère de l'Ecologie et du Développement Durable).*

Successive site visits between 2003 and 2011 showed the development of a chute cutoff on a non-vegetated point bar at a bend near Château de Lys (Fig. 2A). The chute cutoff was initiated in 2004 (Fig. 2B) and remained open for a few years (2009; Fig. 2C). Initially, the chute cutoff developed through a scroll-slough. Later, the chute channel disappeared (2011; Fig. 2D) and observations suggested that two different mechanisms could affect the development of the cutoff. First, migration of the channel upstream led to closure of the chute channel with a plug bar upstream as the inner-bend chute channel received more sediment. Second, high lateral migration rate of the chute channel led to a merge with the outer main channel. Aerial photographs showed that the same bend studied in this paper had multiple scroll-slough cutoffs between 1990 and 2002 as the upstream bend continuously migrated in downstream direction (Table 2, 8–10). Currently, a new scroll-slough cutoff developed at this bend. The chute channel of the scroll-slough cutoff had a small gradient advantage compared to the bend cutoff described above (Table 2, 5–7).

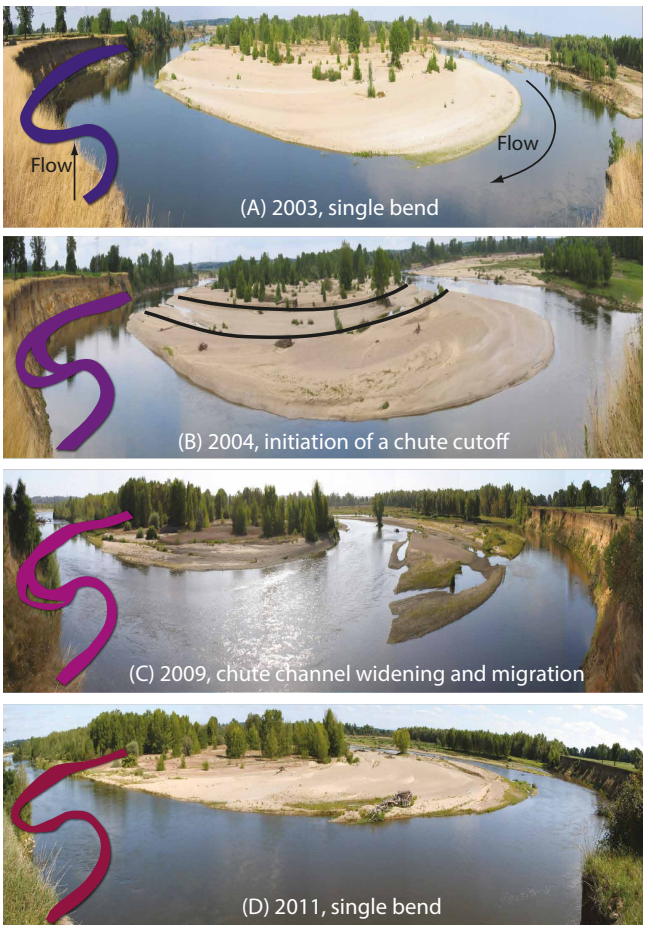

Figure 2: *Oblique images of a meander bend at Château de Lys showing initiation of a chute cutoff and displacement of the chute channel. Images are taken during discharges < 50 m^3/s in (A) August 2003, (B) July 2004, (C) September 2009, and (D) September 2011 (A & B courtesy of M. Baptist).*

Initiation and development of chute cutoffs in the study reach was strongly affected by floodplain characteristics, i.e., sediment composition, floodplain elevation, and the presence of vegetation. The sediment of the river is heterogeneous and consists mostly of gravel with a D_{50} of around 5–8 mm and D_{90} around 9–20 mm depending on the location. During low discharge, below 200 m^3/s, the river bed is covered with a pavement or armouring layer (Kleinhans et al., 2002). Vegetation succession was from pioneer vegetation, herbs, and weeds to softwood forest farther away from the channel. In summer, riparian vegetation, e.g., willows and poplars, developed on the emerged bars (Geerling et al., 2006). This limited the development of bend cutoffs. For example, a sharper bend (Fig. 2A–D) with more softwood in the inner bend decreased chute cutoff initiation over the point bar, whereas on the lower part of the point bar with-

Table 2: *Chute cutoffs observed from aerial images between 1980 and 2008 in the River Allier: chute cutoffs related to a multiple bend cutoff event in 1980 (1–4), bend cutoffs (5–7), and scroll-slough cutoffs (8–10)*

Number	Location	Year	Channel length		Advantage
			Chute (m)	Meander (m)	
1	Chemilly	1980	842	1177	1:1.4
2	Château de Lys	1980	924	1261	1:1.4
3	Le Vizier	1980	1101	1834	1:1.7
4	Bressolles	1980	1062	2082	1:2.0
5	Tilly	1994	551	1769	1:3.2
6	Tilly	2003	801	1847	1:2.3
7	Tilly	2008	890	1653	1:1.9
8	Château de Lys	1994	699	811	1:1.2
9	Château de Lys	2002	454	525	1:1.2
10	Château de Lys	2004	724	1014	1:1.4

out the presence of vegetation a scroll-slough cutoff occurred. Furthermore, several chute cutoffs occurred at a bend with less dense/ young vegetation on the point bar (Fig. 1).

3. Morphodynamic model setup

3.1. Numerical modelling approach

In this study we used two models to understand the development of chute cutoffs. First, we used Delft3D to systematically test scenarios. Delft3D is a physics-based numerical model and simulates hydrodynamics, sediment transport, and morphodynamics and has been used in several fluvial, estuarine, deltaic, and tidal applications (e.g., Lesser et al., 2004; Edmonds and Slingerland, 2008; Kleinhans et al., 2008, 2010; van der Wegen and Roelvink, 2012; Schuurman et al., 2013) and is extensively used and verified in engineering practice. The model schematisation was inspired by the River Allier. We used an initial digital elevation model (DEM) and settings from the River Allier to test scenarios with systematic modifications targeted at chute development for the site where chute cutoffs indeed occur in the prototype. We manipulated the initial settings for controlled model experiments to unravel the bifurcation controls on chute cutoff. To systematically cover general behaviour for a large range of parameters we used the more idealized 1D model of Kleinhans et al. (2011), which is a physics-based research code for partitioning flow and sediment of channels connected at a bifurcation.

3.2. Model description

The Delft3D model (version FLOW 3.60.01.7844, 13 July 2009) computed hydrodynamics, sediment transport, and morphodynamics. For this study we applied a 2D depth-averaged flow field. So, the effects of helical flow driven by flow curvature on bed shear-stress direction were parameterized (Struiksma et al., 1985). Computation of morphodynamics included sediment transport induced by the flow and the longitudinal and transverse bed slope (Struiksma et al., 1985; Lesser et al., 2004; Kleinhans et al., 2008), bank erosion (van der Wegen and Roelvink, 2012), and bed level change because of gradients in sediment transport. Sediment transport was predicted by the Engelund and Hansen (1967) equation. At the inflow boundary, the input of sediment was kept equal to the local sediment transport capacity. Furthermore, we tested a novel method to incorporate bank erosion without cut cell issues (version FLOW 4.00.07.000000, 13 September 2012) using an immersed channel boundary to represent the bank line (Spruyt et al., 2011). Here the shifting bank-lines are followed as separate moving objects on a fixed grid.

The 1D-nodal-point model was set up as three branches connected at a bifurcation node. The model used the nodal point relation described in Kleinhans et al. (2008) to partition flow and sediment, from which morphological development is predicted. One upstream branch is bifurcated in two downstream branches where, at the bifurcation, the flow and sediment partitioning were calculated. Various physical processes were included: backwater effects, transverse bed slope effects, helical flow to simulate the effect of a bend just upstream of the bifurcation, and channel width adjustments whilst conserving mass (Kleinhans et al., 2011). As the downstream branches evolved, the channel width was adjusted to the changing flow discharge partitioning. Besides flow discharge, particle sizes, upstream width, and hydraulic resistance, the most relevant variables for our study were the initial gradient (i.e., the length and elevations above a base level) and the bend radius. We tested the evolution of the branches at the chute bifurcation by varying these two variables for idealized conditions resembling the River Allier, and we ran this 1D model for 5-, 10-, and 50-year periods.

3.3. Model settings

The Delft3D simulations started with an initial topography created from dGPS measurements for the floodplain elevation taken in 2003 and 2004 (data from Baptist, 2005) and aerial images of 2009. The aerial images were used to determine the subaqueous bed elevation, as these were not measured with the dGPS data. Therefore, we used the intensity of the blue colour of the RGB photograph as indication for the water depth (based on Carbonneau et al., 2006). The initial topography was interpolated on a rectangular grid by averaging the collected data, and gaps were interpolated. The grid cells were 11 m long and 8 m wide, which means that the channel width (58–130 m at low flow) is represented by at least five grid cells. The full domain represented an area of 3.96 km in length and 1.67 km in width, so 360 x 208 grid cells. The grid resolution has no effect on the braiding index and the formation of bars in the channel as long as grid size is smaller than bar length and width (Schuurman et al., 2013). The imposed boundary conditions were upstream flow discharge and a single water level specified for the downstream boundary.

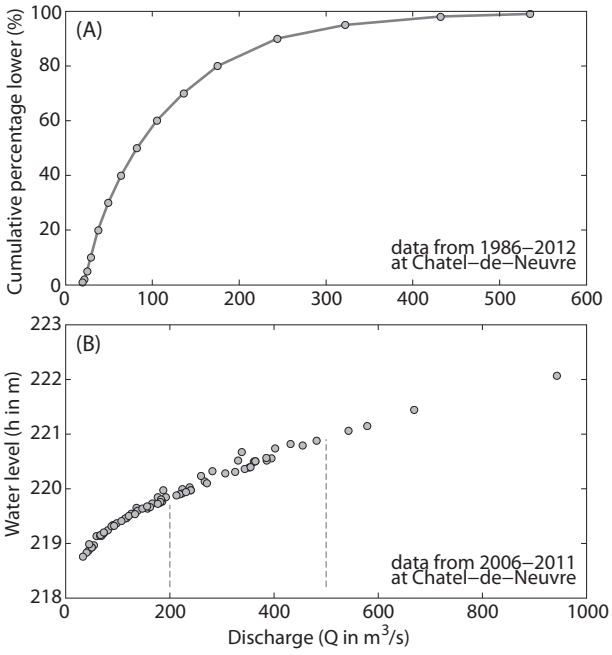

Figure 3: *Discharge regime of the River Allier from the station at Chatel-de-Neuvre, about 10 km upstream of Château de Lys. (A) Cumulative discharge levels for 1986-2012. (B) $Q-h$ relation based on monthly flood levels at Chatel-de-Neuvre from 2006 to 2011. Dashed lines correspond to modelled discharges.*

The simulated time for the flow was five months. The time step of the flow was 0.1 minute, and a 480-minute spin-up interval was applied to stabilize the flow before morphological change was allowed. Assuming that flow was not modified significantly by erosion and sedimentation during one time step, the morphological change in each time step was multiplied by a factor > 1. The chosen morphological acceleration factor was 25. The effect of the factor on bed morphology was usually negligible (Roelvink, 2006; Schuurman et al., 2013). The effect of the morphological acceleration factor is that the 5 months of flow results in a morphological change representing about 10 years.

We specified a median grain size (D_m) of 5 mm and a D_{90} of 9 mm for the entire river section and a constant uniform bed roughness (Nikuradse k_s = 0.15 m). Although the bed roughness in natural rivers varies spatially because of the presence of bedforms, here we used a bed roughness that is based on an average roughness height for the channel. The discharge was kept constant at 200 m^3/s, slightly higher than the mean annual discharge. For some runs we increased the discharge to the annual flood stage of 500 m^3/s. The downstream water level adjustment was based on a $Q-h$ relation of the River Allier based on data from Ministère de l'Ecologie et du Développement Durable (Fig. 3B).

In the 1D model, scenarios were modelled to test the following factors: gradient advantage, i.e., varying the chute channel length, and upstream bend radius (R/W). Other input variables were the same as in the Delft3D settings: the discharge was kept constant at 200 m^3/s, median grain size (D_m) was 5 mm, and bed roughness (k_s) was a constant 0.15 m. Initially, the water discharge was divided between the chute and main channel at a ratio of 1:5. The upstream channel width was 150 m, the same as in the Delft3D simulation at a discharge of 200 m^3/s. We simulated the chute bifurcation development for 5 and 10 years, which is a typical timescale in the River Allier, and for 50 years to assess theoretical equilibrium in otherwise constant conditions. Furthermore, we tested two end members of the shorter channel, i.e., chute channel, located at the inner bend or at the outer bend.

3.4. Sensitivity analysis

To identify and classify the effect of several parameters, we varied several initial and boundary conditions in the Delft3D simulations (Table 3). We tested the effect of an on average 0.8 m higher floodplain elevation at the point bar of interest. Furthermore, we tested the effect of boundary conditions on chute cutoff initiation and development by (i) discharges exceeding the floodplain elevation, (ii) an immersed channel boundary for continuous bend migration upstream instead of a bend cutoff, and (iii) a stronger transverse bed slope effect by changing the calibration factor α from Struiksma et al. (1985), adapted by Talmon et al. (1995):

Table 3: *Tested conditions in Delft3D*

Parameter	Run 1	Run 2	Run 3	Run 4	Run 5	Run 6	Run 7	Run 8	Run 9	
Discharge (Q)	200	200	500	200 500	200	200	200	200	200	(m^3/s)
Sediment size (D_m)	5	5	5	5	5	8	8	8	8	(mm)
Adaptation length of the bed (λ_s)	256	256	503	503	256	157	157	157	157	(m)
Adaptation length of the flow (λ_w)	165	165	308	308	165	211	211	211	211	(m)
Bed roughness (k_s)	0.15	0.15	0.15	0.15	0.15	0.15	0.15	0.15	0.30	(m)
Transverse bed slope (α)	0.7	0.7	0.7	0.7	0.7	0.7	1.0	0.7	0.7	(-)
DEM (original/corrected)	or.	cor.	or.	or.	or.	cor.	cor.	or.	or.	
Immersed outer-bend boundary	no	no	no	no	yes	no	no	no	no	

$$tan\left(\frac{\partial z}{\partial n}\right) = \alpha\sqrt{\theta}\frac{h}{R} \quad (1)$$

where $\partial z/\partial n$ = transverse bed slope, θ (-) is the Shields mobility parameter, h (in m) is water depth, and R (in m) is the radius of streamline curvature. A larger α means a smaller bed slope effect and thus less deflection of the grains by gravity. The transverse bed slope effect has direct implications for vertical bar aggradation, channel width, and bifurcation stability (Bolla Pittaluga et al., 2003; Kleinhans et al., 2008; Nicholas, 2013; Schuurman et al., 2013). We further tested the effect of other parameters: (i) sediment sizes and (ii) bed roughness (Table 3). These parameters were also varied in the 1D-nodal-point model. To evaluate the assumption in the 1D model of equilibrium flow and morphology in bends and to assess the bar regime, we determined the adaptation length of the bed (λ_s) and the adaptation length of the flow (λ_w; Table 3 based on Struiksma et al., 1985). The values for the River Allier predict that alternate bars should form in the channel, which would affect the division of water and sediment at the bifurcation (Miori et al., 2006; Kleinhans et al., 2008). This means that the migration of bars downstream affects the sediment transport division at the bifurcation (Bertoldi et al., 2009).

3.5. Characterization of chute development

The analysis of Wang et al. (1995) is convenient to indicate whether the bifurcation that formed after cutoff is stable or unstable. The Wang et al. (1995) nodal point relation, here only used as indicative, partitions the width-integrated sediment flux of the upstream branch Q_{s1} into the downstream sediment fluxes Q_{s2}, Q_{s3} at bifurcations as:

$$\frac{Q_{s2}}{Q_{s3}} = \frac{Q_2}{Q_3}^{k}\frac{W_2}{W_3}^{1-k} \quad (2)$$

where Q is discharge, W is width of the branch, and k can be determined empirically. This relation

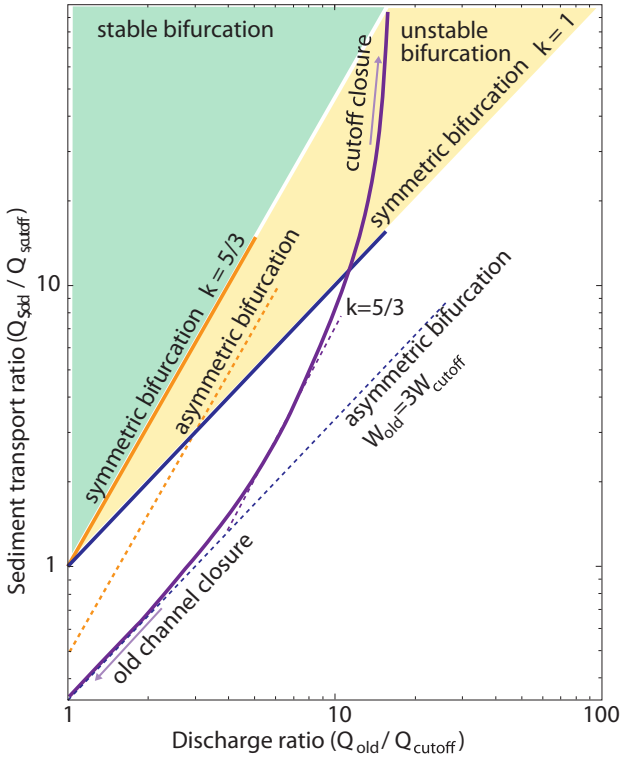

Figure 4: *Conceptual model for bifurcation stability as a function of flow and sediment partitioning (based on Wang et al., 1995). The bifurcations can be stable (green) or unstable (yellow) depending on the value for k (Eq. 2). Bifurcations are asymmetric (dotted lines) if the channel widths of the downstream branches differ. Increasing sediment feed into the old channel indicates closure of the chute channel (purple line toward top), whereas lowering sediment feed results in closure of the old channel (purple line toward bottom).*

allows an effect of nonlinear sediment transport on the partitioning. Usually k is assumed to be 1, e.g., in reduced-complexity models for braided rivers and deltas, which implies that sediment partitioning is proportional to flow discharge partitioning (Kleinhans et al., 2011). However, Wang et al. (1995) found that bifurcations were stable for $k \geq n/3$, where n depends on the transport predictor. We used the equation of Engelund and Hansen (1967) for sediment transport, which means that $n = 5$. In Fig. 4, bifurcations between the drawn lines for $k = 1$ and

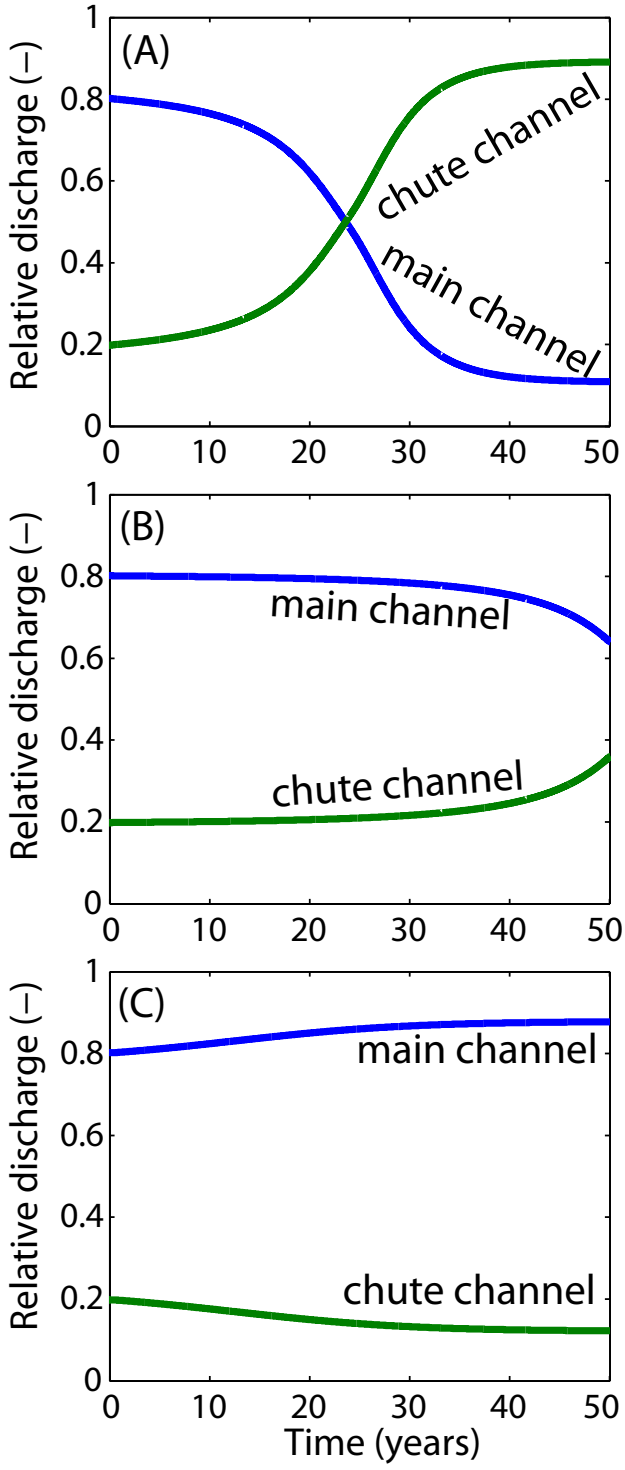

Figure 5: *Results of the 1D-nodal-point model of Kleinhans et al. (2011). (A) Shows the configuration when the chute channel becomes the dominant channel. (B) Shows that the chute and main channels become equally important (nearly symmetrical). (C) Shows that the main and chute channels remain the same over time so that the main channel remains dominant (stable configuration).*

$k < n/3$ are symmetric (as specified) but unstable (blue line and yellow area). Bifurcations with $k > n/3$ are stable (orange drawn line and green area for symmetric cases; Fig. 4). However, incipient chute bifurcations are likely not symmetric, and chute channels may widen and become the dominant channel. Assuming that a chute channel is three times smaller than the main channel, it is asymmetric and the lines for stability shift in the plot (dotted lines, Fig. 4). In practice, modelling shows that the downstream branches evolve (following the purple line, Fig. 4), which leads to initially unstable bifurcations that 'stabilize' with a highly asymmetrical division when one of the downstream branches has nearly closed.

The data obtained from the numerical simulations were reduced to descriptive parameters for development of chute cutoff processes. (i) Bend radius and water depth were extracted upstream of the chute cutoff; and (ii) discharge, sediment transport, water levels, and bed levels were extracted at the branches downstream of the bifurcation. The branches and main channel were identified by thresholding the DEM on a flow velocity of 0.4 m/s, which was a conservative threshold to exclude flow through the inactive swales and on the floodplain. On a fixed cross section upstream of the bifurcation (Fig. 6, locations 1 and 4), the bend radius along the bend was calculated. The cross section upstream of the bifurcation was drawn at about two channel widths upstream of the initial bifurcation. The radius of curvature streamline (R) was calculated as (Fagherazzi et al., 2004):

$$R = \frac{\pi}{2} \frac{\left[\left(\frac{dx}{ds}\right)^2 + \left(\frac{dy}{ds}\right)^2\right]^{3/2}}{\left[\frac{dx}{ds}\frac{d^2y}{ds^2} - \frac{dy}{ds}\frac{d^2x}{ds^2}\right]} \tag{3}$$

where s is the curvilinear streamwise coordinate, which is the calculated streamline for each meter. R is positive (negative) when the bend is turning right (left) for increasing values of s. We used the streamlines based on velocities in x- and y- direction to determine flow direction. Along these streamlines, the distance between upstream of the bifurcation to a specific cross section was measured. The distance was used to determine gradient advantage, which is the gradient of the water level from upstream-of-the-bifurcation (Fig. 6, locations 1 and 4) to the channels downstream (Fig. 6, locations 2/3 and 5/6/7). To determine water discharge, sediment transport, and inlet step between both downstream branches of the bifurcation, the same cross section was used. Furthermore, we measured the bifurcation angle between the chute and main channel at the intersection of the three centrelines.

The 1D model produced the discharge division between both downstream branches over time, showing closure/opening of the main/chute channel (Fig. 5). The outcome showed two types of development; (i) the chute channel rapidly became the dominant channel (Fig. 5A), and (ii) the main channel

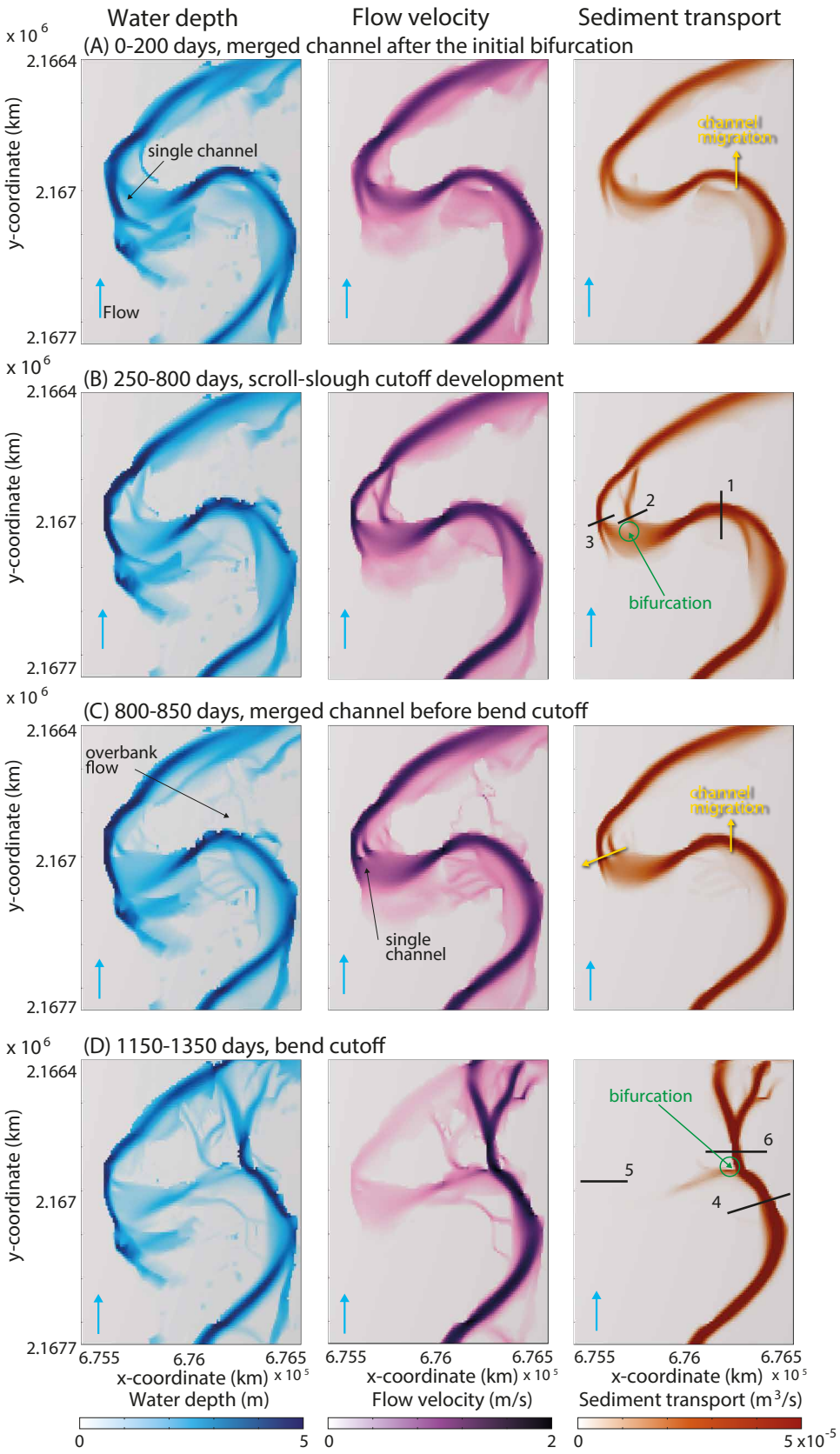

Figure 6: *The development of the channel during run 1. Shown are the water depth, flow velocity, and sediment transport maps. (A) A single thread channel. (B) Scroll-slough cutoff leads to a bifurcation of the bend. Cross section 1 indicates upstream location of the bifurcation. Cross sections 2 and 3 indicate the two downstream branches. (C) Merging of both branches to a single-thread channel again. (D) Bend cutoff, where cross section 4 indicates location upstream of the bifurcation. Cross sections 5 and 6 indicate downstream branches.*

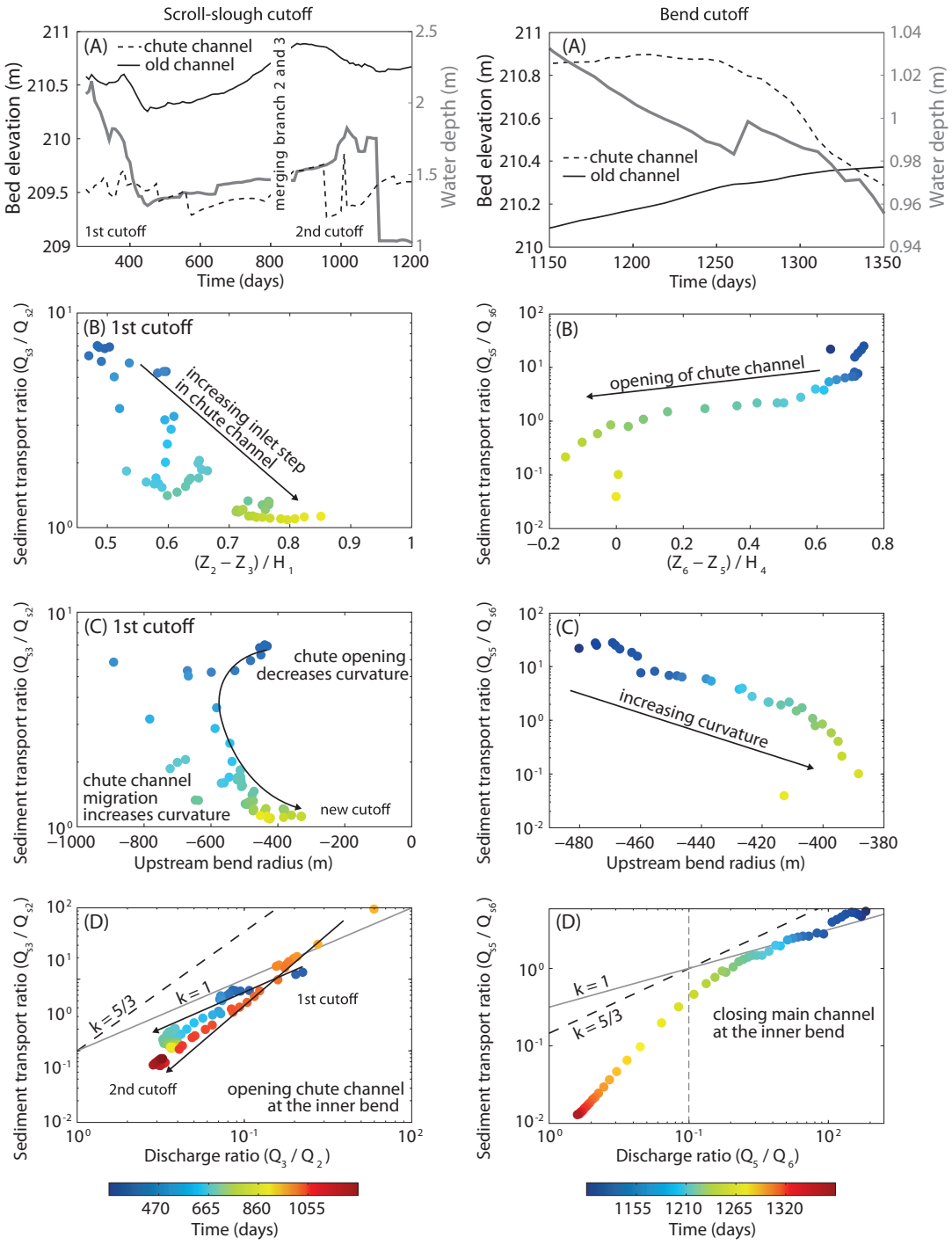

Figure 7: *Scroll-slough cutoff processes (left panel) and bend cutoff processes (right panel) for run 1. (A) Mean bed elevation of the outer channel (Fig. 6, 3,6) and the inner channel (Fig. 6, 2,5) and the water depth upstream of the bifurcation (Fig. 6, 1,4) over time. Sediment transport ratio plotted against (B) inlet step difference between downstream branches, (C) upstream bend radius, and (D) discharge ratio.*

remained the dominant channel (Fig. 5C). For nearly critical conditions, the switch from the main to the chute channel is delayed for a long time (Fig. 5B). The outcome of the 1D model was characterized by the discharge ratio between the inner bend channel and outer bend channel at the end of the run. Negative values indicated that the outer bend channel was dominant, while positive values indicated that the inner bend channel was dominant. Based on 300 runs we empirically determined the line of the transition where either the chute channel or the main channel was dominant for periods of 5, 10, and 50 years.

4. Numerical model outcomes

Here we describe the development of the chute cutoffs for the Delft3D run that had no immersed channel boundary. The effects of initial and boundary conditions and several parameters on the morphodynamics are described in section 4.3.

4.1. General evolution

Several chute cutoffs formed over a period of 10 years, including two scroll-slough cutoffs and one bend cutoff. Initially, the model run reshaped the channel to a morphology related to the constant discharge and led to merging of the two branches in the studied bend (0–200 days; Fig. 6A).

Lateral bend migration increased the channel bend amplitude and length, which later resulted in the development of a scroll-slough cutoff (250–800 days; Fig. 6B). The chute captured the lower swale at the inner side of the bend, which developed during lateral migration of the channel in the first phase. The chute channel was shallow, but significant flow velocities and sediment transport caused incision. The chute channel widened and the channel migrated laterally until both branches merged again (800–850 days; Fig. 6C). Then another scroll-slough cutoff developed, but the development of the chute channel was terminated because of a bend cutoff of the point bar causing bypass (1150–1350 days; Fig. 6D). The bend cutoff started to develop after three years of morphological simulation. Water flow incised a chute channel, and channel widening resulted in a dominant flow through the chute channel, while the former channel was abandoned. Sedimentation at the entrance of the former channel disconnected the channel upstream so that flow velocities reduced and sediment transport through the main channel ceased (Fig. 6D).

4.2. Cutoff development

The development of the meandering river resulted in several cutoffs that together provide a set to explore the roles of the key variables. Here we describe the development of the scroll-slough cutoff and the bend cutoff by descriptive parameters, e.g., bend radius, inlet step, and gradient advantage.

4.2.1 Scroll-slough cutoff

The development of the meander bend increased sinuosity and decreased the bend radius of the bend of interest. Water flow along the inner bend resulted in excavation of a chute channel (Fig. 7A), which resulted in lowering of the water depth (Fig. 7A). The sediment transport through the chute channel was relatively high, which resulted in deposition of sediment and an increase in the inlet step of the chute channel (Fig. 7B, 2) compared to the main channel (Fig. 7B, 3). Eventually, the inlet step rose above the water level and closed the chute channel. Opening of the chute channel resulted in a change in the main flow direction and increased the upstream bend radius (Fig. 7C). Later, bend migration decreased the bend radius again and another scroll-slough cutoff occurred (Fig. 7A). In general, upstream bend radius and water levels above the inlet step controlled initiation and development of the scroll-slough cutoffs. These scroll-slough cutoffs were characterized by a small bifurcation angle of 20–30^o.

The bifurcations were asymmetrical because of different widths of the branches (Fig. 7D). Indeed, the division between water and sediment indicated an unstable bifurcation over time for the first scroll-slough cutoff. The outcome of the Delft3D simulation illustrated that migration of the bifurcation location affected the development of the scroll-slough cutoff. First, the cutoff was initiated at the outer bank, but migration of the bifurcation in a downstream and outward direction led to a shift from outer bend channel to inner bend channel. The end member of the 1D model for a chute channel in the inner bend indicated that despite the gradient advantage of the inner bend channel, the strong curvature upstream of the bifurcation causes closure of the chute channel (Fig. 8A). The second scroll-slough cutoff had a more stable bifurcation initially with the data almost parallel to the line of $k = 5/3$ (Fig. 7D). The chute channel, however, was smaller and the bifurcation was more asymmetric than the first cutoff. The chute channel at the inner side of the bend widened and migrated laterally until merged with the other channel (850 days).

4.2.2 Bend cutoff

The bend cutoff in the middle section of the model resulted in closure of the main channel, while the small cutoff described above resulted in merging of the two downstream branches. The bend cutoff was initiated by a water level rise of only about 0.3 m, which was enough to exceed the floodplain elevation (after 1000 days). The chute channel deepened by incision, whilst sedimentation occurring at the inner side of the bend closed the former channel (Fig. 7A). The incision also caused a drop of the water level. The gradient advantage of the chute channel was considerable as the flow path over the point bar was about 1 km shorter. Longitudinal profiles of both branches showed sedimentation in the main channel (i.e., branch 5), whereas the bed was eroded in the chute channel (i.e., branch 6). A migrated bar upstream in the chute channel resulted in an increase in water level gradient for branch 6, which reduced the gradient advantage during the development of the bend cutoff.

The bend cutoff showed that the inlet step difference between the main channel (Fig. 7D, 5) and the chute channel (Fig. 7D, 6) decreased and that eventually the chute channel became dominant (Fig. 7B). Channel excavation increased the sediment transport through the chute channel. The sediment transport ratio increased significantly for the bend cutoff compared to the bend radius (Fig. 7C). Compared to

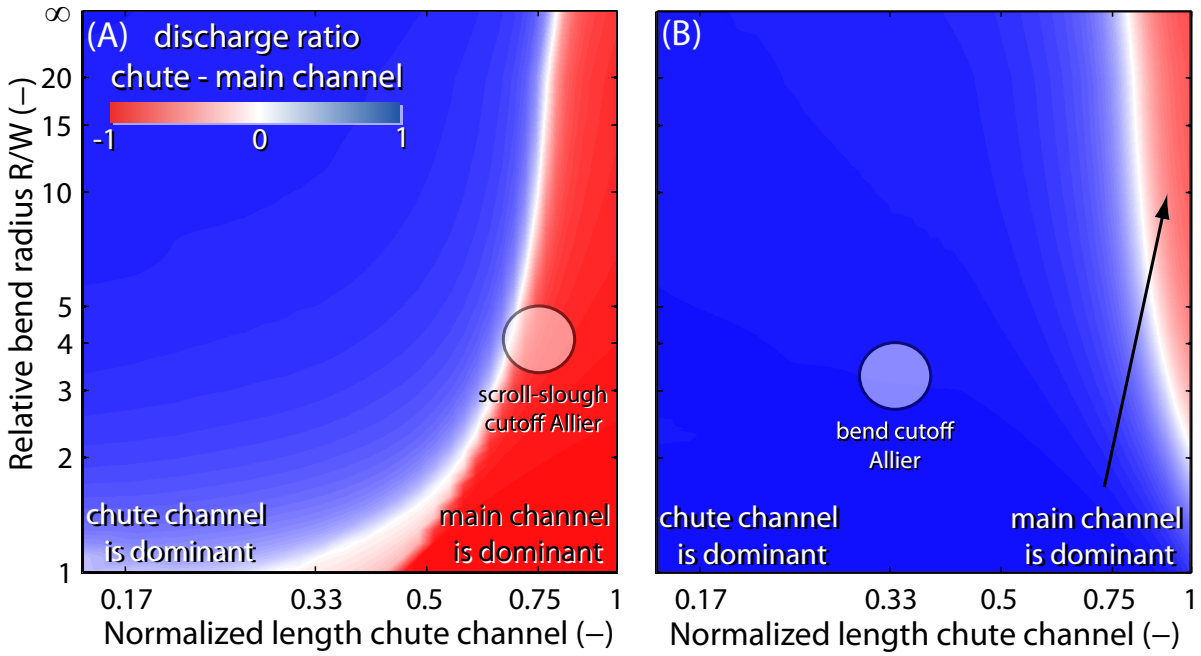

Figure 8: *Chute bifurcation development affected by gradient advantage and bend radius for a chute channel that is located at (A) the inner or (B) the outer bend channel. (A) Sharper bends lead to closure of the shorter chute channel instead of the longer main channel, which is also observed and consistent with the scroll-slough cutoff in the River Allier. (B) Sharper bends lead to faster closure of the main channel, which is also observed and consistent with the bend cutoff in the River Allier.*

the scroll-slough cutoff, the upstream bend radius decrease was insignificant. This suggested that the bend cutoff did not depend on the bend radius. Indeed the 1D model shows that the outer-bend chute channel becomes dominant because of the gradient advantage (Fig. 8B). However, the bend curvature upstream did affect the rate of closure of the main channel: sharper bends led to faster closure. Furthermore, this sharper bend is associated with a larger bifurcation angle of 70–80^o compared to the scroll-slough cutoff .

During initiation of the chute channel, channel widths of the downstream branches differed, causing an asymmetric bifurcation. The resulting asymmetric division of sediment transport and discharge led to excavation of the chute channel and increased the sediment transport through the chute branch (Fig. 7D). The branches temporarily became equal in size, but the bifurcation was unstable with $k = 1$. As the chute channel widened and the main channel closed, a stable bifurcation formed with $k > 5/3$.

These findings show that the development of the two types of cutoffs are controlled by different mechanisms (in agreement with Zolezzi et al., 2012; Grenfell et al., In press). Gradient advantage affected the development of the bend cutoff more than the scroll slough cutoff (Table 4). The floodplain elevation of the bend cutoff was higher compared to the scroll-slough cutoff, making the former less likely than the latter. Furthermore, the inlet step for the bend cutoff lowered, whereas the inlet step for the scroll-slough rose after initialization. This was the result of a sediment transport directed into the inner-bend channel, which led to sedimentation in the scroll-slough, which is the inner-bend channel but deepening of the chute channel in the bend cutoff, where the cutoff is in the outer bend.

4.3. Effect of initial and boundary conditions

We tested the effect of an initial higher floodplain elevation, the effect of boundary conditions (particularly upstream discharge), the immersed channel boundary, and the transverse bed slope effect. We also tested the effects of sediment size and hydraulic roughness on the development of cutoffs in the model runs.

A well-developed point bar (run 2), represented with an artificial higher floodplain, limited the formation of a bend cutoff. An increase of the elevation of the point bar decreased chute excavation (Figs. 9A–B; in agreement with Howard, 1996). This led to more lateral migration of the bend and an increase in sinuosity compared to the run with a lower floodplain. Still, scroll-slough cutoffs developed as these formed on the self-formed point bar, which was lower than the artificial higher floodplain.

Higher discharges, with related higher water levels, promoted the initiation and success of the bend cutoff, while it limited the development of scroll-slough cutoffs. Higher discharges increased water

Table 4: *The range of parameters observed during the scroll-slough and bend cutoff*

Parameters	Scroll-slough	Bend cutoff	Value
Bend radius	300–700	380–480	m
Inlet step	0.5–0.9	-0.2–0.8	m
Gradient advantage	0.5–2.5	4–11	10^{-4} m/m

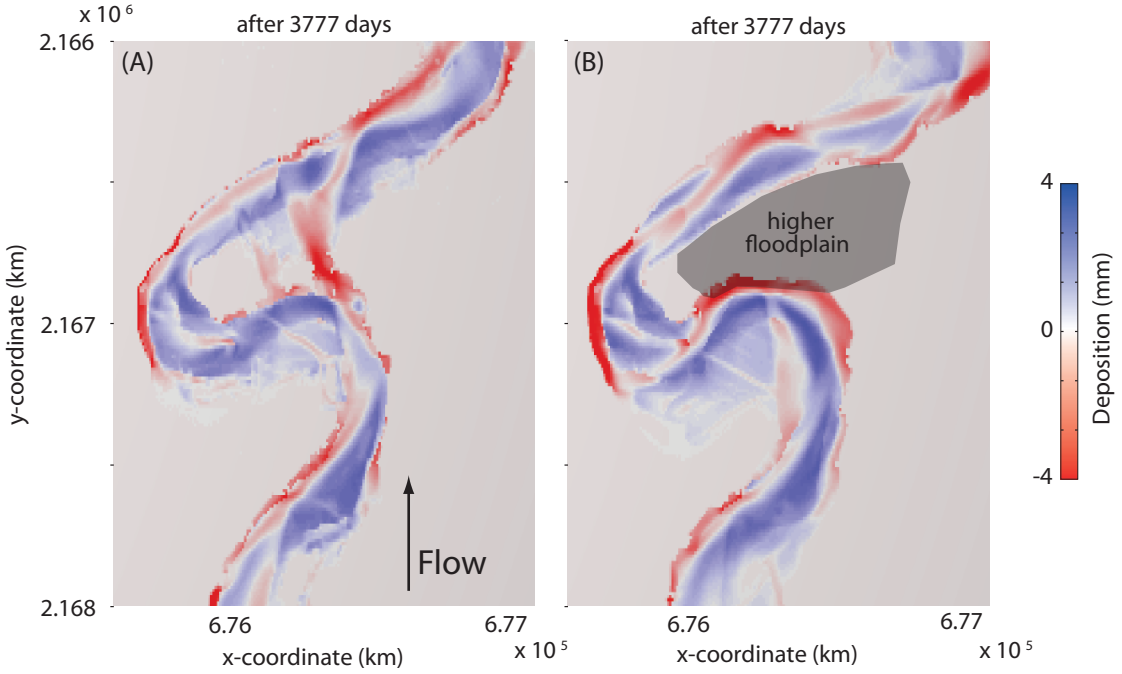

Figure 9: *The effect of floodplain elevation on chute initiation. (A) DEM of difference map for run 1 with a low floodplain as measured with the dGPS. (B) DEM of difference map for run 2 with an artificial higher floodplain (0.8-m increase) at the indicated location.*

levels and resulted in an instant meander bend cutoff. The mean annual flood discharge was sufficient to incise a new channel through the point bar. A simulation with a varying discharge of mean annual discharge (200 m^3/s) for 255 days and mean annual flood discharge (500 m^3/s) for 2 days (run 4) reduced bend cutoff initiation compared to a run with constant discharge of 500 m^3/s (run 3).

The run with an immersed boundary (run 5) led to scroll-slough cutoffs within the bank lines, but the boundary itself limited the development of a bend cutoff. The bank line had to be continuous and could not be divided by a cutoff. The scroll-slough cutoff developed during the same period as in run 1, and after the first scroll-slough cutoff a second one occurred. However, the relation between sediment transport ratio and discharge ratio indicated a more unstable bifurcation compared to run 1 (Fig. 10A). For this case, the chute channel widened and developed to become the dominant channel.

A decreased transverse bed slope effect resulted in narrower but deeper channels (e.g., Schuurman et al., 2013). The transverse bed slope effect was tested on a less dynamic simulation, i.e., coarser grains and higher floodplain elevation. We compared water elevation and channel dimensions between runs with a different transverse bed slope effect; α is 0.7 (run 6) and 1.0 (run 7). Less transverse bed slope effect, i.e., a higher α, resulted in faster lateral migration, so that one more scroll-slough cutoff developed during the same period. Migration rates increased because of deeper channels with higher flow velocities at the outer bank. This led to a shorter bend radius, which promoted the occurrence of the scroll-slough cutoffs. Furthermore, the net flow resistance of narrower and deeper channels flanked by wider, shallower bars increased so that water level rose and inundated a higher floodplain more frequently and caused more scroll-slough cutoffs.

Grain size and bed roughness changed the bifurcation asymmetry and water levels. Increased sediment size led to a decrease in the dynamics and in the number of cutoffs (run 8). Bends became longer and the bend radius did not decrease to critical values for a scroll-slough cutoff. Although dynamics decreased, a bend cutoff developed between 1750 and 2280 days. The development at the bifurcation of the bend cutoff slightly differed between the simulations with different grain sizes. The simulation with the finer bed sediment was more affected by the

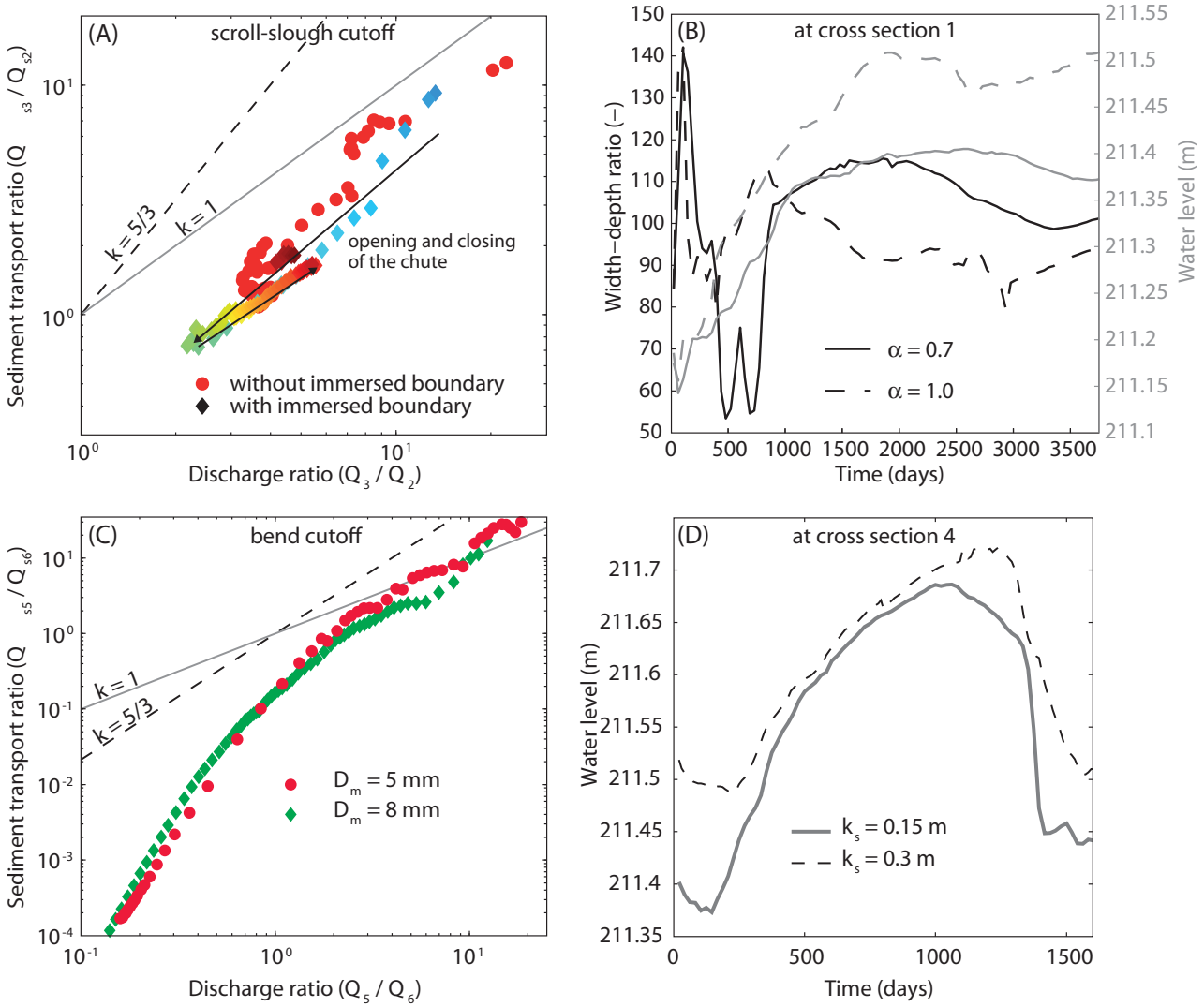

Figure 10: *Sensitivity of key model results to choices in schematization and parameters. (A) Sediment transport ratio compared to discharge ratio for run 5 with and run 1 without an immersed channel boundary for the scroll-slough cutoff. (B)Time series of width-depth ratio and water level for run 6 with α = 0.7 and run 7 with α = 1.0 at cross section 1. (C) Sediment transport ratio and discharge ratio for run 1 with D_m of 5 mm and run 8 with D_m of 8 mm at the bifurcation of the bend cutoff. (D) Time series of water level elevation compared between run 8 with roughness values of k_s = 0.15 m and run 9 with k_s = 0.3 m at cross section 4.*

dominant discharge, so that the sediment transport ratio is higher for the dominant channel than during the coarser bed sediment simulation (Fig. 10C). The coarser bed sediment was less affected by the transverse bed slope because of the lower mobility. Increased bed roughness rose the water level and promoted the occurrence of chute cutoffs (run 9 compared to run 8). Higher water levels resulted in earlier overbank flow and excavation of the chute channel for the bend cutoff (Fig. 10D).

The 1D model outcomes showed that a larger grain size or an increased bed roughness resulted in a shift of the transition between a chute dominant to a main channel dominant bifurcation (Figs. 11A–B). The largest effect was observed when median grain size increased to 8 mm. After 50 years, the runs showed the same transition between chute and main channel dominant bifurcation (Figs. 11A–B), which illustrated that the chute bifurcation is dominantly controlled by the gradient advantage and bend radius. The 50-year scenario showed that the development of the chute became stable later than the 10-year. The 5-year scenario illustrated that the chute channel had not become dominant within the 5 years for several situations. According to the Delft3D run, chute cutoffs occurred within 5 years, which implies that not all chute cutoffs will succeed in natural situations where the upstream and downstream morphology continues to change.

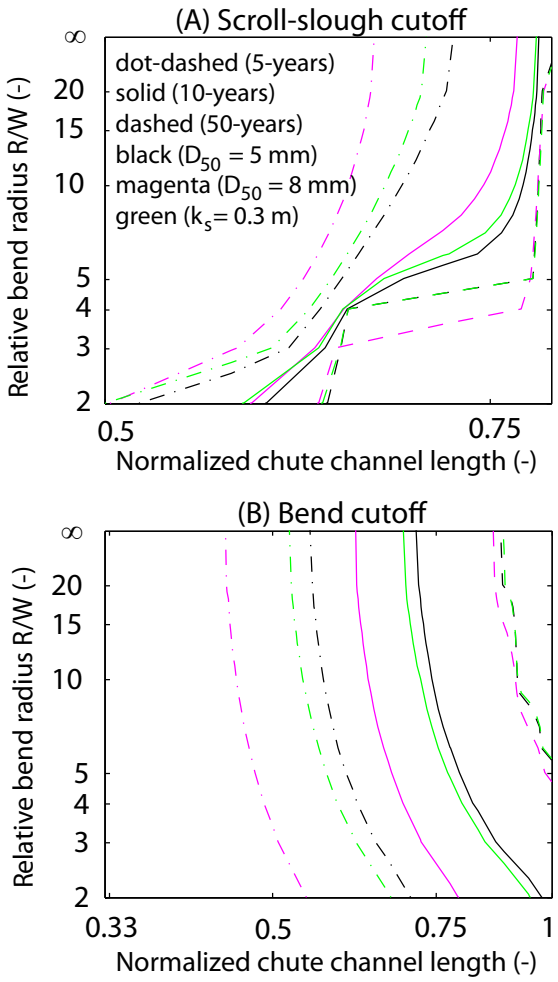

Figure 11: *Simulation time and sensitivity of key model results for an inner-bend chute channel (A) and outer-bend chute channel (B). The effect of simulation time for establishing equilibrium of the chute bifurcation occurs for all settings after 50 years, while increasing grain size and roughness results in less dominance of the chute channel — but after 50 years the transition line is the same.*

These findings illustrated that initiation and development of the channel and the success of chute cutoffs were sensitive to initial conditions and boundary conditions and that many of these have physical meaning. In particular, bend chute cutoff processes were mostly determined by the floodplain elevation. Without flow conditions exceeding the floodplain elevation, bend cutoffs did not occur. Constant discharge was sufficient to obtain overbank flow as channels migrated, but floods were more effective in initiating chute channels — which is not surprising. Water elevation was influenced by the transverse bed slope effect and bed roughness. Grain sizes determined lateral mobility of the channel but did not prevent cutoff processes. The partitioning of sediment at the bifurcation was affected by grain size, transverse bed slope effect, and bend migration upstream, as these determine the sediment transport ratio between both branches.

5. Discussion

5.1. Factors affecting bifurcation evolution at chute cutoffs

This study shows that success or failure of chute cutoffs is largely determined by gradient advantage and channel curvature at the bifurcation, whilst initiation of chute cutoffs is determined by floodwater elevation relative to floodplain elevation and other floodplain characteristics.

The model runs indicate that bifurcations at chute cutoffs in meandering gravel-bed rivers develop to a highly asymmetrical equilibrium, as most discharge is transferred to one of the downstream branches while the other one is closed (in agreement with Wang et al., 1995; Kleinhans et al., 2011). Upstream bends and flow curvature result in helical flow that steers sediment toward the inner channel, whereas discharge is pushed toward the outer channel. So, an upstream channel bend increases asymmetry of sediment and discharge portioning, which leads to sedimentation in the inner channels, which is in agreement with Kleinhans et al. (2008, 2011). Because of sediment transport limitation in the inner channel, a plug bar forms that closes the channel so that inevitably the outer channel wins, as shown in the 1D model. The development of a plug bar was also observed for residual channels in the field (Toonen et al., 2012; Dieras et al., 2013) and in flume experiments (Braudrick et al., 2009; van Dijk et al., 2012).

The gradient advantage and upstream curvature is also observed in the bifurcation angle. In agreement with previous work (Constantine et al., 2010a; Dieras et al., 2013), the bifurcation angle corresponded well with the closure rate of the main branch. Bifurcation angles may affect, or be affected by, relevant fluvial processes. For sharp-bended offtakes, flow separation may occur (Bulle, 1926; Constantine et al., 2010a), and a useful threshold angle for such flow separation may well exist but remains as yet unknown (Blanckaert, 2011). Very sharp bends generally occur when the river banks are strong relative to the flow strength, as is the case in meandering rivers with somewhat cohesive banks or vegetated banks (e.g., Zinger et al., 2013), but not in braided rivers with noncohesive sediment. In more gently curved rivers, the angle asymmetry is therefore an artificial characterisation of the bifurcation planform that are more appropriately described as curved channels (Bridge, 2003). This alternative representation reflects better that flow curvature drives the spiral flow and the resulting transverse sediment flux contribution (Kleinhans et al., 2008).

Initiation and development of the chute cutoff is controlled by several factors. Chute cutoff initiation

occurs when water level exceeds the inlet step or floodplain elevation of the chute channel or point bar, mostly during floods (as shown in Ghinassi, 2011; Zinger et al., 2011). Field observations show that the characteristics of the floodplain, e.g., presence of vegetation, strongly determine the probability of success of chute channel incision. The results show that even with a constant discharge water level could temporarily exceed the floodplain elevation. Factors that lead to fluctuation in the water level are upstream bend radius, transverse bed slope effect, bed roughness, and sediment deposition in the channel. Lateral bend migration shortens the bend radius, which affects the momentum of flow that advects onto and over the point bar in the curved channel (described in Dietrich and Smith, 1983). The transverse bed slope effect determines the width-depth ratio of the channel (e.g., Schuurman et al., 2013), which in turn affects water level and floodplain elevation. The bed roughness increases water levels and promotes overbank flow but does not affect the bifurcation asymmetry and stability as strongly as the transverse bed slope effect.

5.2. Chute cutoffs as an aspect of river patterns

The process of chute cutoffs has been associated with the transition from a meandering to a braiding style (Ashmore, 1991; Kleinhans and van den Berg, 2011; Zolezzi et al., 2012) because the frequent occurrence of cutoffs render a river multichannel and weakly braided by definition and because chute cutoffs are also frequently observed in braided rivers contrary to neck cutoffs. Furthermore, chute cutoffs limit bend growth and channel sinuosity much more severely than neck cutoff, which only occurs in highly sinuous rivers (Howard, 1996). In the example of the River Allier, the event with multiple simultaneous chute cutoffs reduced sinuosity so much whilst creating multiple parallel channels that the river was indeed weakly braided (Kleinhans and van den Berg, 2011).

The development of meandering rivers and the occurrence of chute cutoffs depend on the characteristics of floodplains, in particular bank strength (Ferguson, 1987; Constantine et al., 2010b; Kleinhans, 2010). Weak banks result in channel widening that promotes the formation of mid-channel bars. The process of chute cutoff initiation depends on (i) flood regimes that increase water level, which results in a gradient advantage over the point bar; (ii) bend sinuosity; and (iii) floodplain characteristics, i.e., floodplain elevation, sediment composition, and presence of vegetation. The model results and field observations show that chute cutoffs initiate on the lower or less-developed part of the point bar, mostly at the outer bank. The development of a higher floodplain clearly limits chute initiation in the model run. Furthermore, a stronger and vegetated floodplain would also reduce possibilities for chute initiation (e.g., Braudrick et al., 2009; Nicholas, 2013; van Dijk et al., 2013). Clearly this associates chute cutoffs with weakly meandering rivers with not too strong floodplain development, that is, on the transition from meandering to braiding.

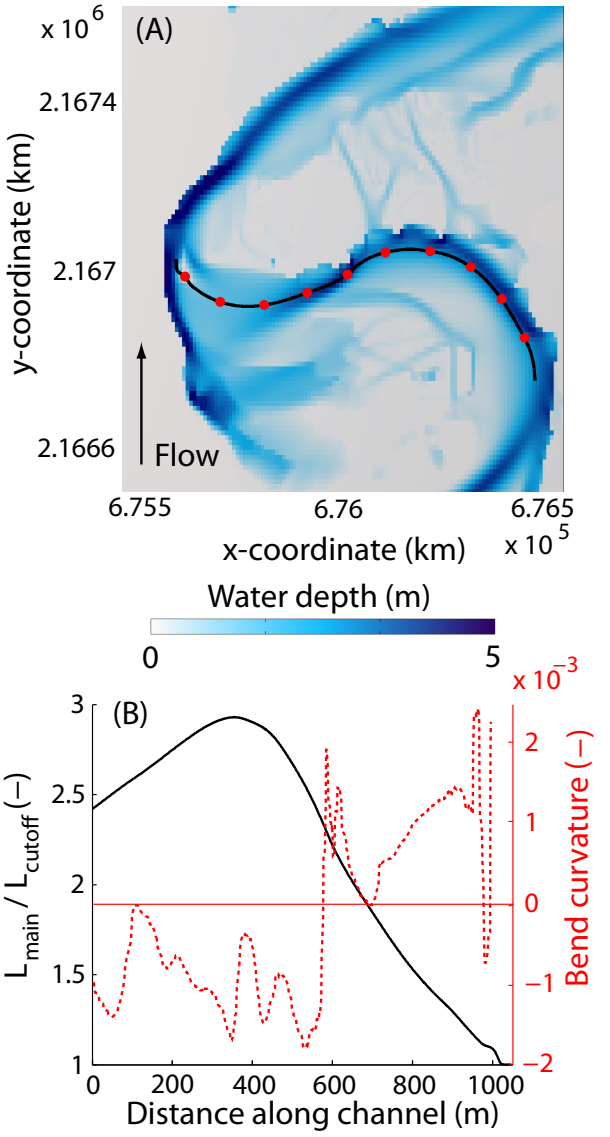

Figure 12: *Curvature of the channel and ratio of the main channel length and cutoff length for the bend in the River Allier. (A) Water depth map and indicated flow path along the main channel. Red dots indicate a distance of 100 m. (B) Length of the channel following the flow path indicated in (A) divided by the shortest path to the downstream part of the channel at the same x location and the bend curvature along the channel.*

The bend cutoffs in the morphodynamic model and field observations of the River Allier are comparable to the chute cutoffs in our experimental meandering river (van Dijk et al., 2012). In the exper-

iment, lateral channel migration and adaptation of the width-depth ratios lead to water level rise and overbank flow across the point bar. The division of flow and sediment results in sedimentation in the inner channel, here the main channel (in agreement with Toonen et al., 2012; Dieras et al., 2013). Sediment mobility in the numerical model is higher compared to experiments, so that a chute channel is excavated before the main channel is closed. In the experiment on the other hand, the main channel was closed before the chute channel was fully excavated (van Dijk et al., 2012). The end-members that are simulated with the 1D model show that bend curvature plays an important role in closure of one of the channels, whereas for less bend curvature as in braided rivers the gradient advantage determines the development of the bifurcation (Schuurman et al., 2013).

The location of the chute cutoff systematically determines the gradient advantage and bend curvature along the bend (Fig. 12A). The length of the main channel is almost three times larger than the shortest flow path over the point bar (Fig. 12B). The bend curvature fluctuates along the bend because of bars, but show a decrease in curvature toward the bend apex and an increase nearing the bend inflections where the sign of curvature changes (Fig. 12B). We observe a scroll-slough cutoff just downstream at the point where the bend starts to curve in the opposite direction. Clearly cutoff development is sensitive to the location of the bifurcation compared to the direction of the curvature upstream.

The morphodynamic model results lead to adaptation of the conceptual model for chute cutoff development based on experiments (van Dijk et al., 2012). Figure 13 illustrates how the two types of chute cutoffs develop depending on bend radius, overbank flow, and floodplain properties. Scroll-slough cutoffs are mostly easier to develop because of a lower floodplain and less vegetation near the channel. The scroll-slough cutoff depends mostly on the radius of the upstream bend and has a lower floodplain, whereas gradient advantage is less for the inner channel. Sediment transport capacity of the chute channel was less than upstream, so that sedimentation leads to lateral migration of the branch, which eventually merges with the outer channel. The lateral migration of the chute channel, however, depends on bar erodibility (e.g., Grenfell et al., 2012, In press). The bend cutoff, on the other hand, is driven by a high gradient advantage between the outer bend and the centre of the channel belt; and this cutoff type therefore requires higher floods to initiate. The presence of vegetation and sediment composition limits the occurrence of bend cutoffs in natural systems (Ferguson, 1987; Constantine et al., 2010b). Here the upstream curvature results in a more asymmetric sediment partitioning compared to discharge partitioning, which likely leads to closure of the main channel (agrees with Miori et al., 2006; Kleinhans et al., 2008). The 1D model outcomes showed that sharper bends (sharper in meandering rivers) played an important role in the success or failure of a chute channel in the river. In other words, scroll-slough cutoffs may occur more frequently and then frequently abandon in favour of the original more sinuous channel, whilst bend cutoffs require rarer floods to form but are more likely to succeed.

5.3. Implications and applications

The understanding of initiation and development for chute cutoffs in gravel-bed meandering rivers also has implications for chute cutoffs in sand-bed meandering rivers. The effect of finer grain size (i.e., sand) mainly affects the transverse bed slope (α; Struiksma et al., 1985; Nicholas, 2013; Schuurman et al., 2013). A reduction in sand size enhances sediment transport in suspension and reduces the sediment transport downward along the transverse bed slope. This would lead to vertical bar growth, steering of the flow — which eventually leads to narrower sinuous channels — and larger bifurcation angles (Nicholas, 2013; Schuurman et al., 2013). This effect was also apparent in the sensitivity analysis where we reduced the transverse bed slope effect (increased α), which resulted in deeper but narrower channels and higher migration rates (in agreement with Schuurman et al., 2013). However, the number of scroll-slough cutoffs increases because of higher sediment mobility. This and other evidence suggests that a sustained, single-thread, sand-bed meandering river must have floodplains that are more cohesive or strengthened by vegetation so that bank erosion rate as well as the number of chute cutoffs decreases.

Howard (1996) proposed a probability function to predict the occurrence of chute cutoffs in his model so that sinuosity is reduced and the planform presents a more realistic sinuosity. Here the probability of a chute cutoff depends on five properties: namely gradient, distance, floodplain elevation, planimetric angle between the former and chute channel, and the near-bank velocity. Using a reduced complexity model, Howard (1996) showed — by varying the coefficient for each property — that sinuosity is mostly affected by the ratio of gradient, distance across the potential chute, and the elevation of the floodplain, which is corroborated with our results. The novel result of our work is that upstream bend radius and bend adjustment affect the success of a chute cutoff. This process in particular is to be included for meandering rivers, where relative bend radius has more effect compared to braided rivers. Furthermore, the channel morphology (e.g., transverse bed slope, bed roughness and grain sizes) affects the local water level and the occurrence of chute cutoffs.

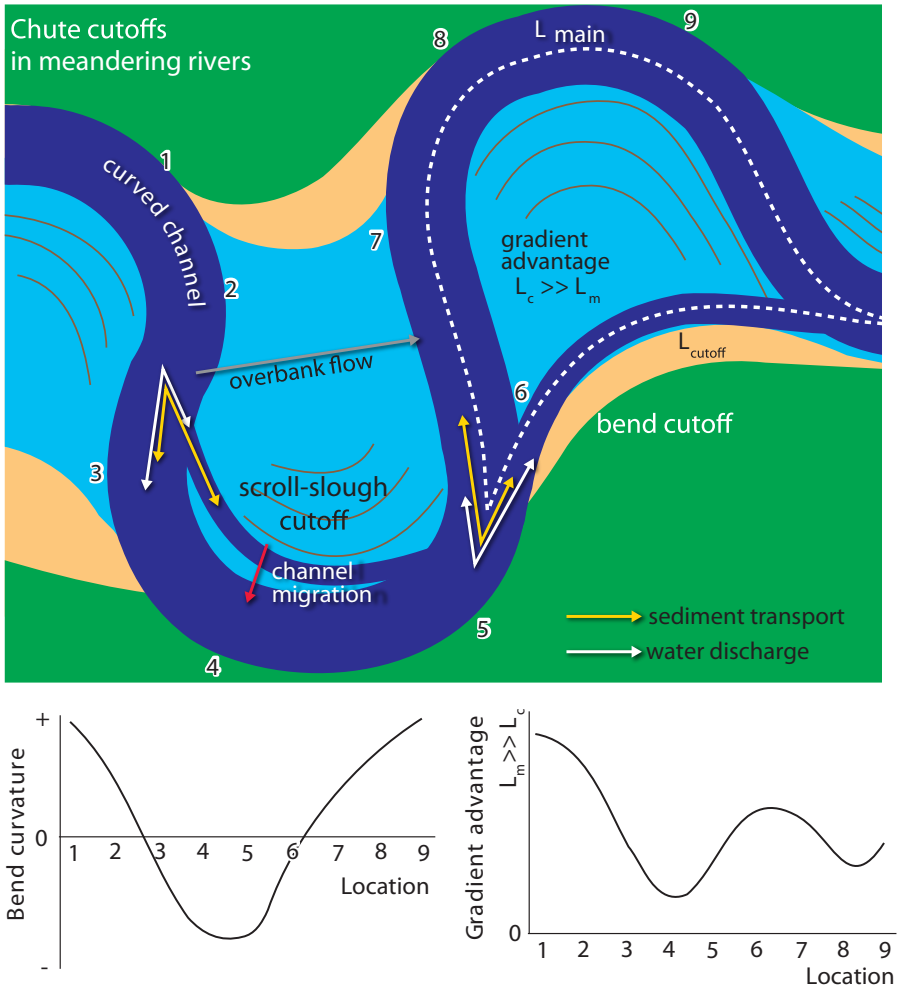

Figure 13: *Conceptual model describes the development of chute cutoffs in a meandering gravel-bed river. Scroll-slough cutoffs formed when bend radius decreased. A bend cutoff developed because of a gradient advantage. The graphs indicate the bend curvature and gradient advantage along the meander bend where the location is indicated by a number. Limitations in the development of a cutoff are the floodplain characteristics, i.e., floodplain elevation, sediment composition, and the presence of vegetation.*

Chute cutoff occurrence and behaviour has implications for understanding sedimentary architecture as well as the dynamics of physical habitats. Frequent chute cutoff reduces the meander belt width (Howard, 1996; van Dijk et al., 2012), which is important for planning meandering river restoration projects and affects channel belt and thus potential reservoir width. Repetitive chute cutoffs rework point bars, which reduces preservation of large-scale inclined strata; whereas residual channel fills flanking the channel belt are more likely to preserved (Lewin and Macklin, 2003; van de Lageweg et al., 2013). The process of chute cutoff behaviour significantly affects the dynamics of a stream, which is essential to create physical habitats. Continuous opening and closure of scroll-slough cutoffs result in increasing environmental severity; whereas the bend cutoff leads to abandonment and formation of oxbow lakes, which are the 'hot spot' providing habitat for numerous plant and wildlife species (Ward et al., 1999; Piégay et al., 2000).

6. Conclusions

We studied controls on the initiation and development of chute cutoffs in meandering gravel-bed rivers. During chute channel development, the channel splits into the old channel and the chute. We analysed and modelled the effects of factors known to be important for river bifurcations, particularly gradient advantage and channel curvature just upstream of the bifurcation. Two types of chute cutoffs occur: scroll-slough cutoffs and bend cutoffs. We conclude that chute *initiation* depends on floodplain characteristics, i.e., floodplain elevation, sediment composition and the presence of vegetation. Chute cutoff *success* or *failure* is determined by the dynamics just upstream of the channel bifurcation and location of the chute channel in the bend that determines channel curvature and gradient advantage. Systematic scenario modelling shows that:

• Chute cutoffs are initiated by flow over the point bar when the water level is sufficiently high, which

even occurs during a constant discharge when local water impoundment can lead to locally high water levels.

• Field observations show that initiation and development of chute cutoff depend on floodplain characteristics, in particular the elevation. Furthermore, riparian vegetation on the point bar decreases chute incision.

• Upstream bend radius and curvature affect local water level and initiate cutoffs when bends become sharper. The scroll-slough cutoffs form on low point bars with limited vegetation.

• Gradient advantage promotes initiation of a bend cutoff over the point bar and the abandonment of the old main channel and thus local avulsion. The gradient advantage for the bend cutoff is higher than for scroll-slough cutoffs.

• Sediment partitioning is much more asymmetric than discharge partitioning. Upstream bends result in helical flow that steers sediment toward the inner channel. So that, a plug bar develops at the inner bend channel.

• Relative bend radius determines the success of closure of one downstream branch, which is important for sustaining a meandering river. A sharper bend increases closure rate for shorter outer bend channels, whereas for shorter inner bend channels the plug bar leads to failure of a cutoff.

• The water level is influenced by the transverse bed slope effect and bed roughness, whereas grain size, transverse bed slope effect, and upstream bend migration determine water discharge and sediment load partitioning at the bifurcation.

Acknowledgments

WMvD, FS, and MGK were supported by the Netherlands Organisation for Scientific Research (NWO) (grant ALW-Vidi-864·08·007 to MGK). WIvdL was supported by Exxon Mobil Upstream Research (grant EM01734 to MGK and G. Postma). We thank Janrik van den Berg for guiding us to the river Allier and for insightful discussions, and thank Martin Baptist for providing dGPS data and images of the River Allier. Comments on an earlier draft and discussion by Hans Middelkoop greatly helped to improve the paper. We acknowledge the anonymous reviewer for comments that significantly improved the manuscript and editor Richard Marston for their helpful guidance.

References

Ashmore, P.E., 1991. How do gravel-bed rivers braid? Canadian J. of Earth Sciences 28, 326–341.

Baptist, M.J., 2005. Modelling floodplain biogeomorphology. Ph.D. thesis, TU Delft, Delft University of Technology, The Netherlands.

Bertoldi, W., Zanoni, L., Miori, S., Repetto, R., Tubino, M., 2009. Interaction between migrating bars and bifurcations in gravel bed rivers. Water Resources Research 45, W06418. doi:10.1029/2008WR007086.

Blanckaert, K., 2011. Hydrodynamic processes in sharp meander bends and their morphological implications. Journal of Geophysical Research 116, F01003. doi:10.1029/2010JF001806.

Bolla Pittaluga, M., Repetto, R., Tubino, M., 2003. Channel bifurcation in braided rivers: equilibrium configurations and stability. Water Resources Research 39, 1046. doi:10.1029/2001WR001112.

Braudrick, C.A., Dietrich, W.E., Leverich, G.T., Sklar, L.S., 2009. Experimental evidence for the conditions necessary to sustain meandering in coarse bedded rivers. Proceedings of the National Academy of Sciences of the United States of America 106, 16936–16941. doi:10.1073/pnas.0909417106.

Bridge, J., 2003. Rivers and Floodplains. Blackwell, Oxford, UK.

Bulle, H., 1926. Untersuchungen über die Geschiebeableitung bei der Spaltung von Wasserläufen. Forschungsarbeiten auf dem Gebiete des Ingenieurwesens Heft 282, 57–84. (in German)

Carbonneau, P.E., Lane, S.N., Bergeron, N.E., 2006. Feature based image processing methods applied to bathymetric measurements from airborne remote sensing in fluvial environments. Earth Surface Processes and Landforms 31, 1413–1423. doi:10.1002/esp.1341.

Constantine, J.A., Dunne, T., Piégay, H., Kondolf, G.M., 2010a. Controls on the alluviation of oxbow lakes by bed-material load along the Sacramento River, California. Sedimentology 57, 389–407. doi:10.1111/j.1365-3091.2009.01084.x.

Constantine, J.A., McLean, S.R., Dunne, T., 2010b. A mechanism of chute cutoff along large meandering rivers with uniform floodplain topography. Geological Society of America Bulletin 122, 855–869. doi:10.1130/B26560.1.

Dieras, P.L., Constantine, J.A., Hales, T.C., Piégay, H., Riquier, J., 2013. The role of oxbow lakes in the off-channel storage of bed material along the Ain River, France. Geomorphology 188, 110–119. doi:10.1016/j.geomorph.2012.12.024.

Dietrich, W.E., Smith, J.D., 1983. Influence of the point bar on flow through curved channels. Water Resources Research 19, 1173–1192.

Edmonds, D.A., Slingerland, R.L., 2008. Stability of delta distributary networks and their bifurcations. Water Resources Research 44, W09426. doi:10.1029/2008WR006992.

Engelund, F., Hansen, E., 1967. A Monograph on Sediment Transport in Alluvial Streams. Teknisk Forlag, Kobenhavn, Denmark.

Fagherazzi, S., Gabet, E.J., Furbish, D.J., 2004. The effect of bidirectional flow on tidal channel planforms. Earth Surface Processes and Landforms 29, 295–309. doi:10.1002/esp.1016.

Federici, B., Paola, C., 2003. Dynamics of channel bifurcations in noncohesive sediments. Water Resources Research 39, 1162. doi:10.1029/2002WR001434.

Ferguson, R.I., 1987. Hydraulic and sedimentary controls of channel pattern. In: Richards, K. (Ed.), River Channels: Environment and Process. Blackwell, Oxford, UK, pp. 129–158.

Fisk, H.N., 1947. Fine-grained Alluvial Deposits and Their Effects upon Mississippi River Activity. Waterways Experiment Station, Vicksburg, MS.

Gay, G.R., Gay, H.H., Gay, W.H., Martinson, H.A., Meade, R.H., Moody, J.A., 1998. Evolution of cutoffs across meander necks in Powder River, Montana, USA. Earth Surface Processes and Landforms 23, 651–662.

Geerling, G., Ragas, A., Leuven, R., van den Berg, J., Breedveld, M., Liefhebber, D., Smits, A., 2006. Succession and rejuvenation in floodplains along the river Allier (France). Hydrobiologia 565, 71–86.

Ghinassi, M., 2011. Chute channels in the Holocene high-sinuosity river deposits of the Firenze plain, Tuscany, Italy. Sedimentology 58, 618–642. doi:10.1111/j.1365-3091.2010.01176.x.

Grenfell, M., Aalto, R., Nicholas, A., 2012. Chute channel dynamics in large, sand-bed meandering rivers. Earth Surface Processes and Landforms 37, 315–331. doi:10.1002/esp.2257.

Grenfell, M.C., Nicholas, A.P., Aalto, R., In press. Mediative adjustment of river dynamics: the role of chute channels in tropical sand-bed meandering rivers. Sedimentary Geology. doi:10.1016/j.sedgeo.2013.06.007.

Hardy, R.J., Lane, S.N., Yu, D., 2011. Flow structures at an idealized bifurcation: a numerical experiment. Earth Surface Processes and Landforms 36, 2083–2096. doi:10.1002/esp.2235.

Hooke, J.M., 2003. Coarse sediment connectivity in river channel systems: a conceptual framework and methodology. Geomorphology 56, 79–94. doi:10.1016/S0169-555X(03)00047-3.

Howard, A.D., 1996. Modeling channel evolution and floodplain morphology. In: Anderson, M.G., Walling, D.E., Bates, P.D. (Eds.), Floodplain Processes. John Wiley and Sons Ltd, Chichester, UK, pp. 15–65.

Kleinhans, M.G., 2010. Sorting out river channel patterns. Progress in Physical Geography 34, 287–326. doi:10.1177/0309133310365300.

Kleinhans, M.G., van den Berg, J.H., 2011. River channel and bar patterns explained and predicted by an empirical and physics-based method. Earth Surface Processes and Landforms 36, 721–738. doi:10.1002/esp.2090.

Kleinhans, M.G., Wilbers, A., Swaaf, A.D., van den Berg, J., 2002. Sediment supply-limited bedforms in sand-gravel bed rivers. J. of Sedimentary Research 72, 629–640.

Kleinhans, M.G., Jagers, H.R.A., Mosselman, E., Sloff, C.J., 2008. Bifurcation dynamics and avulsion duration in meandering rivers by one-dimensional and three-dimensional models. Water Resources Research 44, W08454. doi:10.1029/2007WR005912.

Kleinhans, M.G., Weerts, H., Cohen, K., 2010. Avulsion in action: reconstruction and modelling sedimentation pace and upstream flood water levels following a Medieval tidal-river diversion catastrophe (Biesbosch, The Netherlands, 1421–1750 AD). Geomorphology 118, 65–79. doi:10.1016/j.geomorph.2009.12.009.

Kleinhans, M.G., Cohen, K.M., Hoekstra, J., IJmker, J.M., 2011. Evolution of a bifurcation in a meandering river with adjustable channel widths, Rhine delta apex, The Netherlands. Earth Surface Processes and Landforms 36, 2011–2027. doi:10.1002/esp.2222.

Kleinhans, M.G., De Haas, T., Lavooi, E., Makaske, B., 2012. Evaluating competing hypotheses for the origin and dynamics of river anastomosis. Earth Surface Processes and Landforms 37, 1337–1351. doi:10.1002/esp.3282.

Kleinhans, M.G., Ferguson, R.I., Lane, S.N., Hardy, R.J., 2013. Splitting rivers at their seams: bifurcations and avulsion. Earth Surface Processes and Landforms 38, 47–61. doi:10.1002/esp.3268.

Lesser, G.R., Roelvink, J.A., Van Kester, J.A.T.M., Stelling, G.S., 2004. Development and validation of a three-dimensional morphological model. Coastal Engineering 51, 883–915. doi:10.1016/j.coastaleng.2004.07.014.

Lewin, J., Macklin, M.G., 2003. Preservation potential for Late Quaternary river alluvium. Journal of Quaternary Science 18, 107–120. doi:10.1002/jqs.738.

Lewis, G.W., Lewin, J., 1983. Alluvial cutoffs in Wales and the Borderlands. In: Collinson, J.D., Lewin, J. (Eds.), Modern and Ancient Fluvial Systems. Blackwell Publishing Ltd., Oxford, UK, pp. 145–154. doi:10.1002/9781444303773.ch11.

Marston, R.A., Girel, J., Pautou, G., Piégay, H., Bravard, J., Arneson, C., 1995. Channel metamorphosis, floodplain disturbance and vegetation development: Ain River, France. Geomorphology 13, 121–131. doi:10.1016/0169-555X(95)00066-E.

McGowen, J., Garner, L., 1970. Physiographic features and stratification types of coarse-grained point bars: modern and ancient examples. Sedimentology 14, 77–111.

Micheli, E.R., Larsen, E.W., 2011. River channel cutoff dynamics, Sacramento River, California, USA. River Research and Applications 27, 328–344. doi:10.1002/rra.1360.

Miori, S., Repetto, R., Tubino, M., 2006. A one-dimensional model of bifurcations in gravel-bed channels with erodible banks. Water Resources Research 42, W11413. doi:10.1029/2006.

Nicholas, A., 2013. Morphodynamic diversity of the world's largest rivers. Geology 41, 475–478. doi:10.1130/G34016.1.

Piégay, H., Bornette, G., Hérouin, E., Moulin, B., Statiotis, C., 2000. Channel instability as a control on silting dynamics and vegetation patterns within perifluvial aquatic zones. Hydrological Processes 14, 3011–3029.

Roelvink, J.A., 2006. Coastal morphodynamic evolution techniques. Coastal Engineering 53, 277–287. doi:10.1016/j.coastaleng.2005.10.015.

Schuurman, F., Marra, W.A., Kleinhans, M.G., 2013. Physics-based modeling of large braided sand-bed rivers: bar pattern formation, dynamics and sensitivity. Journal of Geophysical Research.118, 2509–2527. doi:10.1002/2013JF002896.

Spruyt, A., Mosselman, E., Jagers, H.R.A., 2011. A new approach to river bank retreat and advance in 2D numerical models of fluvial morphodynamics. In: RCEM 2011: Proceedings of the 7th IAHS Symposium of River, Coastal and Estuarine Morphodynamics, Tsinghua University Press, Beijng, China, pp. 1863–1871.

Struiksma, N., Olesen, K.W., Flokstra, C., De Vriend, H.J., 1985. Bed deformation in curved alluvial channels. Journal of Hydraulic Research 23, 57–79. doi:10.1080/00221688509499377.

Talmon, A., Struiksma, N., van Mierlo, M., 1995. Laboratory measurements of the direction of sediment transport on transverse alluvial-bed slopes. Journal of Hydraulic Research 33, 495–517.

Toonen, W.H.J., Kleinhans, M.G., Cohen, K.M., 2012. Sedimentary architecture of abandoned channel fills. Earth Surface Processes and Landforms 37, 459–472. doi:10.1002/esp.3189.

van de Lageweg, W.I., van Dijk, W.M., Kleinhans, M.G., 2013. Channel belt architecture formed by a meandering river. Sedimentology 60, 840–859. doi:10.1111/j.1365-3091.2012.01365.x.

van der Mark, C.F., Mosselman, E., 2013. Effects of helical flow in one-dimensional modelling of sediment distribution at river bifurcations. Earth Surf. Proc. Landf. 38, 502–511. doi:10.1002/esp.3335.

van der Wegen, M., Roelvink, J.A., 2012. Reproduction of estuarine bathymetry by means of a process-based model: Western Scheldt case study, the Netherlands. Geomorphology 179, 152–167. doi:10.1016/j.geomorph.2012.08.007.

van Dijk, W.M., van de Lageweg, W.I., Kleinhans, M.G., 2012. Experimental meandering river with chute cutoffs. Journal of Geophysical Research 117, F03023. doi:10.1029/2011JF002314.

van Dijk, W.M., Teske, R., van de Lageweg, W.I., Kleinhans, M.G., 2013. Effects of vegetation distribution on experimental river channel dynamics. Water Resources Research 49, 7558–7574. doi:10.1002/2013WR013574.

Wang, Z., Fokkink, R., de Vries, M., Langerak, A., 1995. Stability of river bifurcations in 1D morphodynamic models. Journal of Hydraulic Research 33, 739–750.

Ward, J.V., Tockner, K., Schiemer, F., 1999. Biodiversity of floodplain river eecosystem: ecotones and connectivity. Regulated Rivers: Research & Management 15, 125–129.

Zinger, J.A., Rhoads, B.L., Best, J.L., 2011. Extreme sediment pulses generated by bend cutoffs along a large meandering river. Nature Geoscience 4, 675–678. doi:10.1038/NGEO1260.

Zinger, J.A., Rhoads, B.L., Best, J.L., 2013. Flow structure and channel morphodynamics of meander bend chute cutoffs: a case study of the Wabash River, USA. Journal of Geophysical Research.118, 2468–2487. doi:10.1002/jgrf.20155.

Zolezzi, G., Bertoldi, W., Tubino, M., 2009. Morphological analysis and prediction of river bifurcations. In: Sambrook Smith, G.H., Best, J.L., Bristow, C.S., Petts, G.E. (Eds.), Braided rivers: Processes, Deposits, Ecology and Management. Blackwell Publishing Ltd., Oxford, UK, pp 233–256. doi:10.1002/9781444304374.ch11.

Zolezzi, G., Luchi, R., Tubino, M., 2012. Modeling morphodynamic processes in meandering rivers with spatial width variations. Reviews of Geophysics 50, RG4005. doi:10.1029/2012RG000392.